J. Chem. Sci. Vol. 125, No. 4, July 2013, pp. 859–867.

Synthesis, characterization and photo-epoxidation performance of Au-loaded photocatalysts

VAN-HUY NGUYEN, HSIANG-YU CHAN and JEFFREY C S WU*
Department of Chemical Engineering, National Taiwan University, Taipei 10617, Taiwan
e-mail: cswu@ntu.edu.tw

MS received 7 November 2012; revised 11 February 2013; accepted 5 April 2013

Abstract. Titanium silicalite-1 (TS-1) was synthesized by hydrothermal crystallization. Au-loaded TS-1 (Au/TS-1) was prepared by the photo-deposition method. The prepared photocatalysts have been fully characterized by Raman, Brunauer–Emmett–Teller (BET), transmission electron microscopy, scanning electron microscopy, X-ray diffraction, X-ray photoelectron spectroscopy, and ultraviolet visible light spectroscopy to reveal their structure, surface morphology and chemical composition. Photocatalytic activity of these photocatalysts was ascertained by gas phase photo-epoxidation of propylene-to-propylene oxide in the presence of molecular oxygen only under light irradiation. No sacrificial reductant such as hydrogen was used during the photoreaction. Au/TS-1 photocatalyst remained highly stable under reaction conditions. It is found that the increased Ti^{3+} sites due to the incorporation of Au will not only enhance the selectivity of the photocatalyst to form epoxide but also its stability during C_3H_6 conversion.

Keywords. Photo-epoxidation; propylene oxide; molecular oxygen; Au-loaded photocatalyst; titanium silicalite (TS-1).

1. Introduction

For the last 60 years, the demand for chemicals worldwide has reached an unprecedented level as development of the third world countries continues. For instance, propylene oxide (PO), the second-most valuable chemical intermediate, has become increasingly important to the chemical industry.[1–3] It has been estimated that the global PO consumption reached 6.0 million tons (2009) from 3.9 million tons (1991). An annual average growth of over 7% was forecasted from 2009 to 2014 as demand recovered after the economic crisis.[4]

$$CH_3CHCH_2 + O_2 + H_2 \xrightarrow[\text{high temp., high pressure}]{\text{Thermocatalyst}} CH_3CHCH_2O + H_2O \quad (1)$$

It is realized that propylene epoxidation with H_2–O_2 mixture using mesoporous and nanoporous Ti support modified by noble metals such as Au and Ag has received more and more attention due to its excellent catalyst stability as well as activity (eq. 1).[5–10] Earlier efforts using Au/TiO_2 catalyst by Hayashi *et al.*[6] have demonstrated high selectivity (>90%) towards PO at low propylene conversion (∼1%) at 303–393 K. Cumaranatunge and Delgass[7] found that Au-loaded titanium silicalite-1 (Au/TS-1) catalyst can improve the reactivity which achieved 5–10 % propylene conversion with a selectivity of 75–85 % towards PO at 473 K. However, it is important to mention that the extra thermal energy needed for the reaction and the safety concern of hydrogen will make such a route only a provisional solution.

$$2CH_3CHCH_2 + O_2 \xrightarrow[\text{mild conditions}]{\text{Photocatalyst}} 2CH_3CHCHC_2O \quad (2)$$

Recently, there is an increasing interest in the direct gas-phase photocatalytic epoxidation (eq. 2).[11–15] In this approach, the concept of green chemistry, the most desirable process, is adopted in which light energy is

*For correspondence

used as a driving force to activate the epoxidation reaction in the presence of molecular oxygen only. Photo-epoxidation process holds the key for sustainable development because it has several advantages such as low energy consumption, free pollutant emission, and generation of eco-friendly end products since the process can be activated by photons at ambient temperature.

Much effort has been devoted to improve selective photo-epoxidation by using noble metal loaded photocatalyst in mild conditions. Recently, we have reported the use of TS-1 photocatalyst to promote photo-epoxidation of propylene using only molecular oxygen in a flow reactor system.[11] In this study, Au-loaded TS-1 and TiO_2 were synthesized and fully characterized by Raman, BET, transmission electron microscopy (TEM), scanning electron microscopy (SEM), X-ray diffraction (XRD), X-ray photoelectron spectroscopy (XPS) and ultraviolet visible light spectroscopy (UV-vis). Selective photo-epoxidation of propylene was performed over P25, TS-1, Au/TiO_2 and Au/TS-1 with only molecular oxygen.

2. Experimental

2.1 *Preparation of photocatalysts*

TS-1 support material was synthesized according to the literature.[16] Basically, it was obtained from hydrothermal crystallization of gel which was formed from the reaction of tetraethylorthosilicate (TEOS, Aldrich, 98%) and titanium (IV) tetrabutoxide (TBOT, Alfa Aesar, 98%) in the presence of tetrapropylammonium hydroxide (TPAOH, 20% in water, Fluka).

Au-loaded photocatalysts were prepared by photo-deposition method, which was adopted by Yang *et al.*[17] TS-1 and Degussa P25 titania were used as support photocatalysts. First, $HAuCl_4$ solution and support photocatalysts were mixed together and adjusted to pH=5.5 by using 0.1 M of Na_2CO_3. Then, 200-W mercury-arc lamp (filter: 320–500 nm, intensity: 0.1 W.cm^{-2}) was used to irradiate the mixture for 120 min with stirring. The photo-deposition reaction was conducted under room temperature to avoid aggregation of gold.[18] The Au loading was 0.5 and 0.1 wt% for TiO_2 and TS-1 photocatalysts, respectively. The colour of the solution, initially deep purple, became clear after photo-deposition indicating that Au was almost loaded on TiO_2 and TS-1. Finally, the mixture was filtered and washed in de-ionized water before drying in an oven at 393 K and calcining in air at 773 K for 5 h.

2.2 *Photocatalyst characterization*

The prepared photocatalysts were fully characterized by powder XRD (X-ray-M03XHF, Ultima IV) to verify their crystalline structure. All XRD peaks were checked and assigned to known crystalline phases. Light absorption of the photocatalyst was revealed by UV-vis (Varian Cary-100). $BaSO_4$ was used as a standard baseline sample. XPS was carried out on the Thermo Theta Probe instrument to determine the chemical composition of the photocatalyst and the chemical state of various species. SEM was conducted on the Nova Nano SEM 230 instrument. TEM was performed on the Hitachi H-7100 electron microscope instrument. BET surface area was measured with the Micromeritics, ASAP 2000. Raman spectra of the photocatalysts were obtained by the single-monochromator Renishaw Raman System 1000 equipped with a thermoelectrically cooled charge coupled device (CCD) detector (−73°C) and holographic edge filter. The samples were excited with 514-nm Ar line. Spectral resolution was 2 cm^{-1}, and spectrum acquisition time was 300 s for each sample.

2.3 *Photo-epoxidation reaction*

Figure 1 shows the apparatus for carrying out photo-epoxidation of propylene-to-propylene oxide. First, 0.02 g of photocatalyst was packed in a photo-reactor with a quartz window for light transmission. The UV-A (320–500 nm) in 200-W mercury-arc lamp was used as the irradiation source and guided to the photo-reactor by an optical fibre. The photo-reactor was placed on a hot plate in case heating was required. The reaction was carried out with a reactant gas mixture

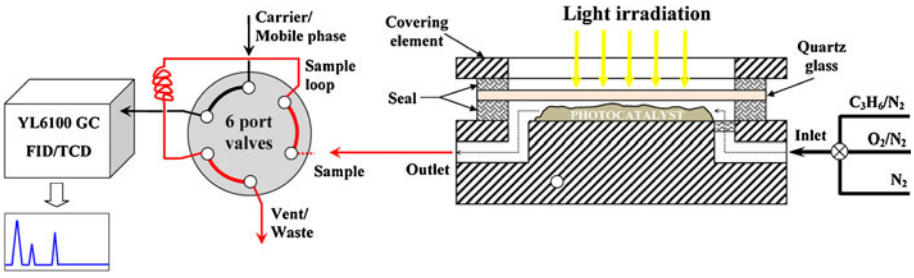

Figure 1. Apparatus for gas-phase photocatalytic epoxidation of propylene.

of C_3H_6:O_2:N_2=1:1:18, and GHSV=6,000 h^{-1}. The stream was analysed online and periodically using a gas chromatograph (Young Lin, YL6100 GC) equipped with a flame ionization detector (FID), a thermal conductivity detector (TCD) and both Molecular Sieve-5A and Porapak-N columns. Propylene conversion rate and product selectivity in the reaction were calculated directly by eqs (3) and (4) as defined below.

$$C_3H_6\text{conv. rate} = \sum \text{rate of products converted to } C_3 \quad (3)$$

$$\text{Product selectivity} = 100\% \times \text{product converted to } C_3 / \text{all products converted to } C_3 \quad (4)$$

3. Results and discussion

3.1 *Photocatalyst characterization*

3.1a *Morphology and crystal structures*: Crystalline structure of the photocatalysts was identified by using XRD. In figure 2(a), photocatalysts containing TiO_2 show obvious XRD peaks corresponding to anatase and rutile phase as expected in P25. The obtained diffraction patterns as seen in figure 2(b) are consistent with those reported in literature.[11,16] The presence of single diffractive peaks at $2\theta = 24.3^\circ$ in the XRD pattern indicates a change from monoclinic symmetry of Silicalite-1 (S-1) to orthorhombic symmetry of titanium silicalite-1 (TS-1). The 2θ values at which major peaks appear for both Au–TiO_2 and Au/TS-1 are found to be almost the same as those of P25 and TS-1, respectively, except for the intensities of the peaks. It suggests that loading of Au does not affect crystal structure, but it may alter crystallinity of the photocatalysts. In addition, no peak corresponding to gold can be observed from XRD analysis. This may be explained by the fact that Au concentration used in this study is extreme low ($\leq 0.5\%$), making the signal of gold peaks too weak to be detected.

Figure 3 shows Raman spectra of P25, Au/TiO_2, TS-1 and Au/TS-1 photocatalysts when excited by

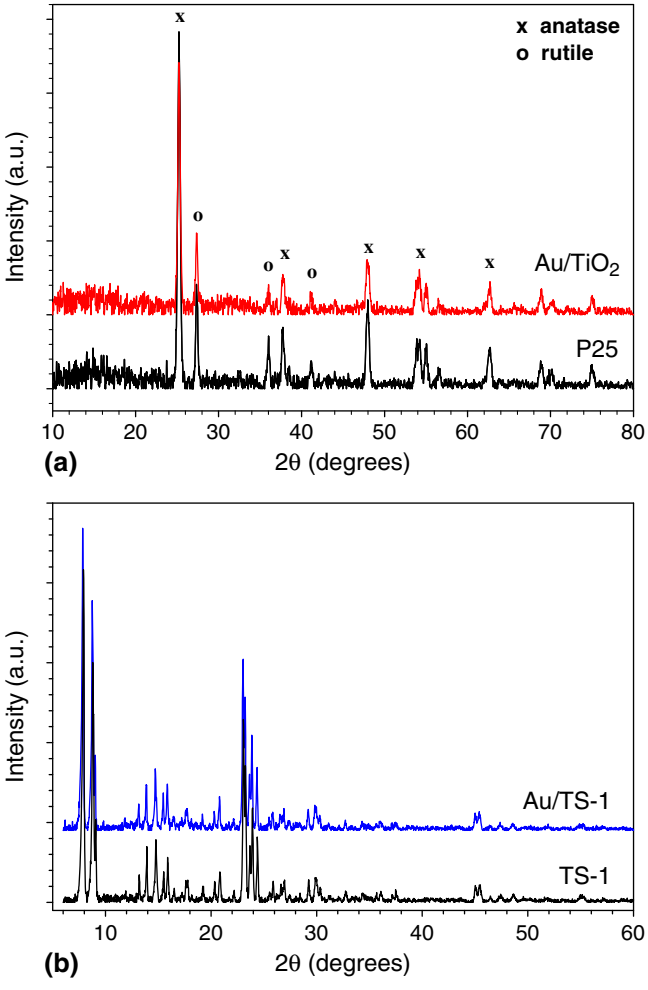

Figure 2. X-ray diffraction patterns of photocatalysts: (**a**) P25 and Au/TiO_2; (**b**) TS-1 and Au/TS-1.

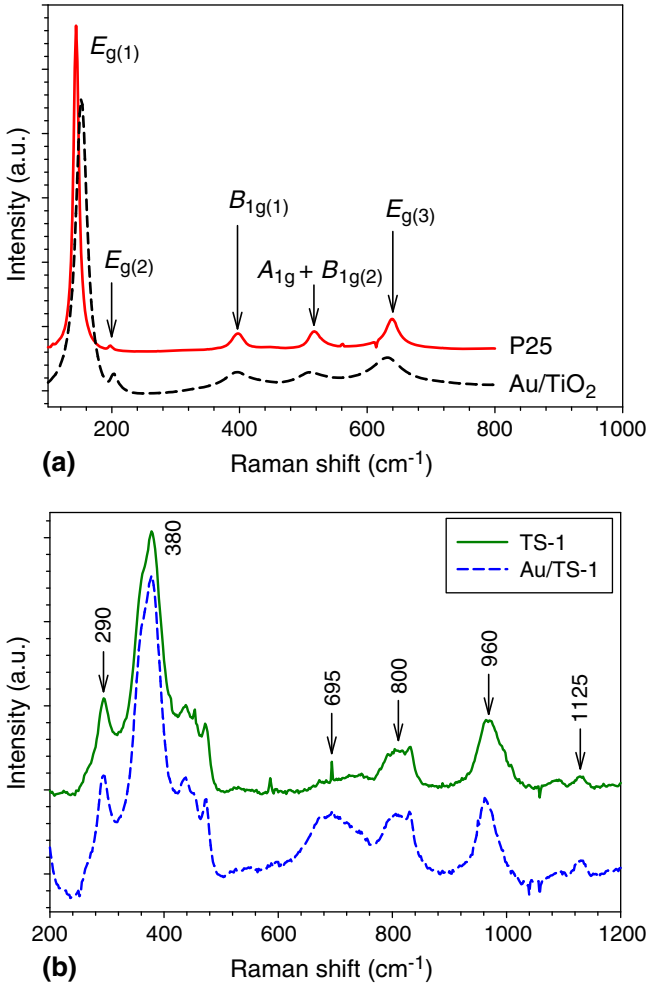

Figure 3. Raman spectra of photocatalysts: (**a**) P25 and Au/TiO_2; (**b**) TS-1 and Au/TS-1.

wavelength of 514 nm. Figure 3(a) shows the presence of six Raman-active fundamentals in the vibrational spectrum: three E_g modes centred around 149, 201 and 638 cm^{-1} (designated here $E_{g(1)}$, $E_{g(2)}$ and $E_{g(3)}$, respectively), two B_{1g} modes at 396 and 514 cm^{-1} (designated $B_{1g(1)}$ and $B_{1g(2)}$), and an A_{1g} mode at 514 cm^{-1}.[19] Figure 3(b) shows Raman spectrum of Au/TS-1, which is almost identical to that of TS-1. Both of them show the characteristic Raman bands of MFI structures (290, 380 and 800 cm^{-1}) and two Ti-specific bands (960 and 1125 cm^{-1}), typically found for TS-1. Among the two Ti-specific bands, the 1125 cm^{-1} band corresponds to the totally symmetric stretching mode of the $[Ti(OSi)_4]$ unit, while the 960 cm^{-1} band is a combination of three asymmetric stretching modes of the same unit.[20] The Raman results further confirm that loading of Au does not affect crystal structure of TS-1 and TiO_2 supports, which is consistent with the XRD results.

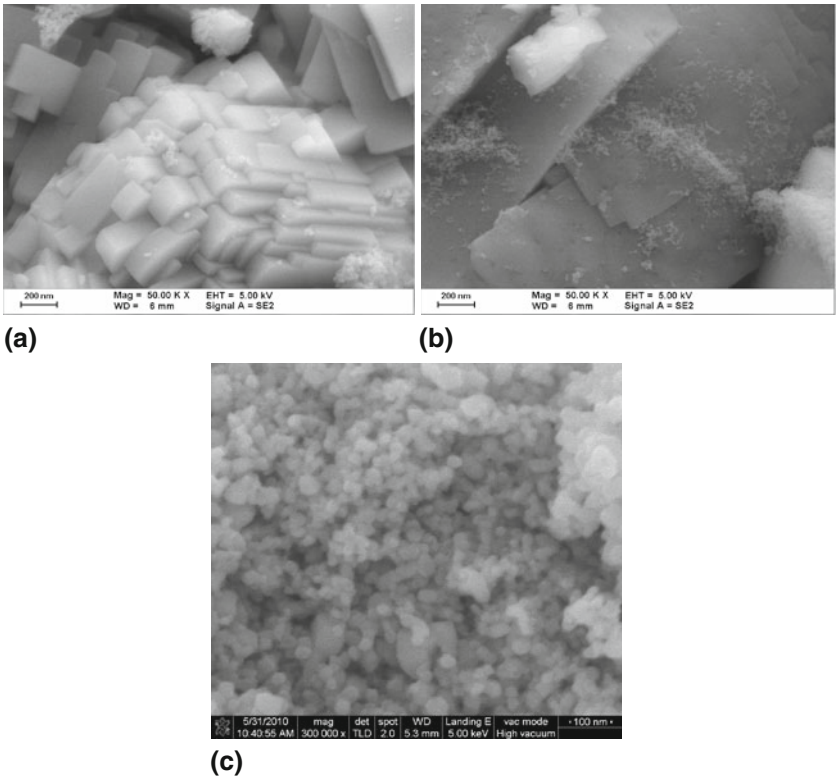

Figure 4. SEM micrographs of photocatalysts: (**a**) TS-1, (**b**) Au/TS-1 and (**c**) Au/TiO_2.

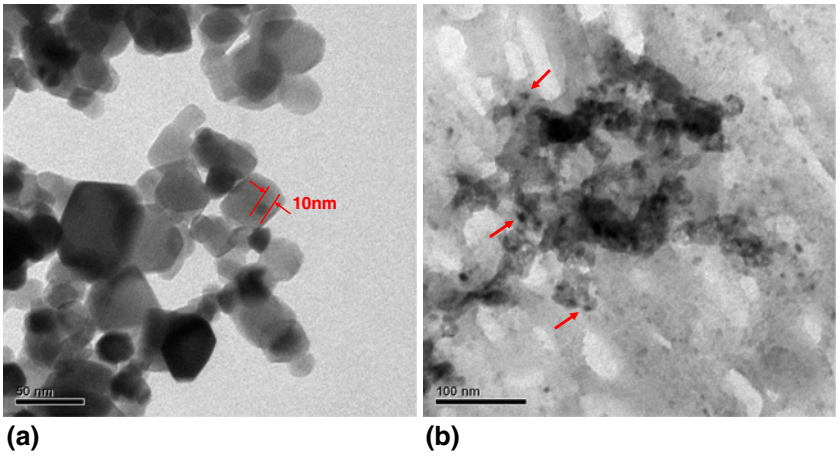

Figure 5. TEM micrographs of photocatalysts: (**a**) Au/TiO_2 and (**b**) Au/TS-1.

Table 1. Results of propylene photo-epoxidation over various photocatalysts.[a]

Entry	Catalysts	Au loading (wt%)	BET ($m^2.g^{-1}$)	C_3H_6 conv. rate[b] ($\mu mol.g^{-1}.h^{-1}$)	PO formation rate ($\mu mol.g^{-1}.h^{-1}$)	Selectivity[c] (%)					
						AA	PO	PA	AC	ROH	CO_2
1	P25	–	50.0	130.0	0.13	5.3	0.1	1.1	5.9	0.2	87.4
2	Au/TiO_2	0.5	47.6	141.8	1.56	14.8	1.1	1.1	7.5	0.4	75.1
3	TS-1	–	369	54.2	23.67	21.5	43.7	26.9	7.9	ND	ND
4	Au/TS-1	0.1	377	56.1	30.35	12.7	54.3	27.1	5.9	ND	ND

[a]The data is the mean value obtained on stream after 12 h (except 4 h for entries 1 and 2) | Reaction conditions: feed gas, C_3H_6:O_2:N_2=1:1:18 in vol.% at GHSV=6,000 h^{-1}, light intensity: 0.1 $mW.cm^{-2}$ (except 0.2 $mW.cm^{-2}$ for entries 1 and 2); reaction temperature: 323 K (except 298 K for entry 1) | PO: Propylene oxide; PA: Propionaldehyde; AC: Acetone; AA: Acetaldehyde | ND: not detected.

[b]C_3H_6 conversion rate = $\sum$ rate of all products converted to C3

[c]$\text{Product selectivity} = \dfrac{100\% \times \text{mol of the formation product converted to } C_3}{\text{mol of all products converted to } C_3}$

Figure 4(a) and (b) shows the SEM micrograph of TS-1 and Au/TS-1 photocatalyst, respectively, indicating that small amount of TiO_2 is aggregated on the SiO_2 surface in some regions. Figure 4(c) shows the SEM micrograph of Au/TiO_2 with the average particle size of roughly 20 nm for TiO_2.

TEM was used to identify Au particles loaded on both TiO_2 and TS-1 photocatalysts in this study. From the TEM results shown in figure 5, Au particles are observed on both TiO_2 and TS-1. The dark-field TEM image reveals that Au particles were dispersed in TiO_2 and TiO_2 matrix of TS-1 with a mean particle size of 10–12 nm.

The BET surface areas of TS-1 and TiO_2 support materials, before and after depositing Au, are shown in table 1. Au loading on these supports does not bring any significant change in their surface areas.

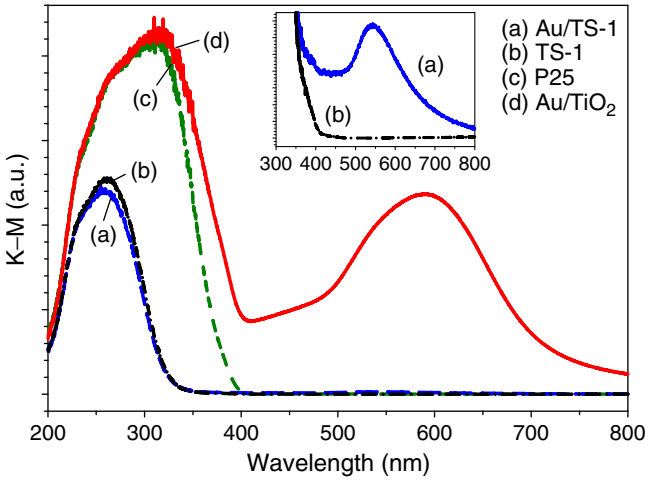

Figure 6. UV-vis absorption spectra of photocatalysts.

3.1b *UV-vis analysis*: UV-vis absorption spectra of different photocatalysts are shown in figure 6. P25 is a commercial TiO_2 photocatalyst that absorbs only UV light (< 380 nm). Au loading on TiO_2 photocatalysts significantly affects the light absorption property of bare TiO_2, i.e., the appearance of an absorption band ranging from 500 to 700 nm, which is attributed to surface plasmon resonance (SPR) effect of noble metals.[21] Spectra of TS-1 supports with the absorption at about 200–400 nm are widely used to confirm the presence of isolated Ti(IV) in the framework position as well as the extra-framework titanium-containing species.[11,22] For the spectrum of Au/TS-1, a small peak corresponding to SPR is also observed (inset of figure 6).

The band gap of TS-1 and Au/TS-1 photocatalyst is calculated by extrapolating the absorption edge onto the energy axis. First, the absorption data is fitted to equations for both direct and indirect band gap transitions. Figure 7(a) shows the $[F(R)hv]^2$ versus hv plot for a direct transition and figure 7(b) shows the $[F(R)hv]^{1/2}$ versus hv plot for an indirect transition, where $F(R)$ is the absorption coefficient, hv=(1239/λ) eV is the photon energy, and λ is the wavelength (nm). The value of hv extrapolated to $F(R)$=0 gives an absorption energy, which corresponds to a band gap E_g. As seen in figure 7(a) for direct transition, both TS-1 and Au/TS-1 show a perfect fit and the extrapolation yields band gap (E_g) values of 4.01 and 4.06 eV, respectively. On the other hand, the band gap estimated from the less-perfect-fit indirect transition is 3.56 and 3.51 eV for TS-1 and Au/TS-1, respectively. Reddya *et al.*[23] suggested that a direct band gap transition would result in a more efficient absorption of solar energy.

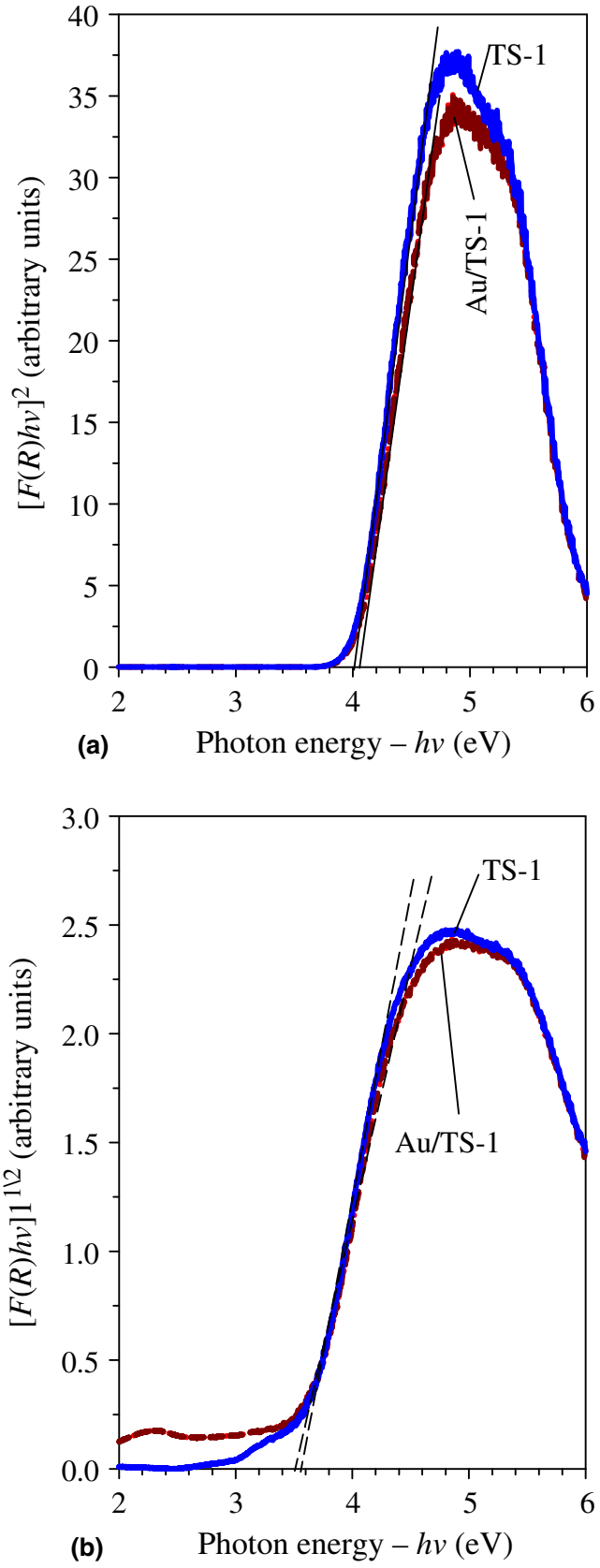

Figure 7. (**a**) Plot of $[F(R)hv]^2$ versus hv for direct transition and (**b**) Plot of $[F(R)hv]^{1/2}$ versus hv for indirect transition. Band gaps E_g are obtained by extrapolation to $F(R) = 0$.

3.1c *XPS analysis*: Figure 8 shows Ti 2p and Si 2p XPS spectra of both Au/TS-1 and TS-1 photocatalysts before and after photoreaction. It can be seen that these two samples before and after the reaction have shown identical surface chemical composition, suggesting that the photocatalysts are highly stable during the photoreaction.[11] Figure 9 shows Ti 2p XPS spectra for the photocatalysts. For TS-1 support, peaks corresponding to the transitions of Ti $2p_{1/2}$ and Ti $2p_{3/2}$ are clearly observed. The oxidation state for Ti $2p_{1/2}$ and Ti $2p_{3/2}$ are 3+ and 4+, respectively, with the former assigned to extra-framework titania and the latter to framework titanium.[24,25] There is a significant amount of Ti in the oxidation state of 3+ rather than the oxidation state of 4+ observed in the Ti 2p XPS spectra of Au/TS-1 (67.4 %) and TS-1 (49.5 %) photocatalysts. Sinha *et al*.[26] mentioned that molecular oxygen can be taken up by a Ti^{3+} cation site (Ti^{4+}–O–Au^0 ↔Ti^{3+}–O–Au^+) and is activated to a negatively charged molecular oxygen species. Hence, the loading of Au on TS-1 in this study can increase the amount of Ti with oxidation state of 3+ in TS-1, favouring selective photo-epoxidation. It suggests that reduced titanium species is crucial in photo-efficiency, in agreement with the result in previous studies on photo-degradation of methyl orange and phenol.[25] Furthermore, it is worth mentioning that the Ti^{3+} sites in photocatalysts are highly stable in air under irradiation, which will not induce any activity degradation.[27] This further supports the highly stable photo-activity results observed in this study. The XPS spectrum of Au 4f was also measured; however, no peak corresponding to Au 4f was detected. This may be due to the weak signal, which is lower than the detection limit of the XPS (∼1% detection limit).

3.2 *Photocatalytic epoxidation of propylene*

We re-assessed the direct gas-phase photo-epoxidation of propylene via molecular oxygen by using various kinds of photocatalysts. From the results, no activity was observed either in the absence of photocatalysts with UV-irradiation or with photocatalysts in the absence of UV-irradiation, confirming that the epoxidation that occurs over photocatalysts is mainly photocatalytic epoxidation.

Table 1 summarizes the product formation rate and product selectivity. It was interesting to find that Au loading not only promoted the conversion rate of propylene but also improved the selectivity of epoxide formation in the photocatalytic epoxidation. Among the photocatalysts tested, Au/TS-1 shows the best performance. The PO formation rate of Au/TS-1 is

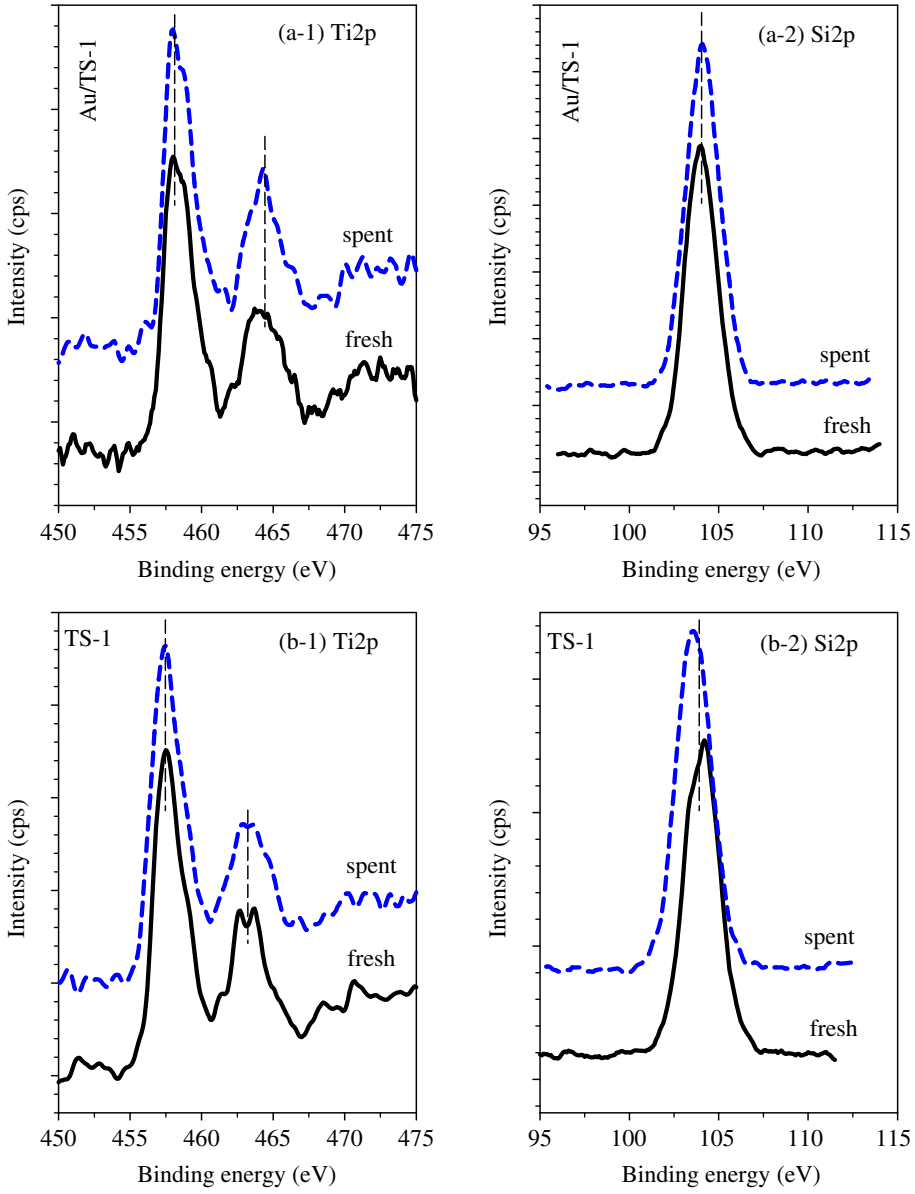

Figure 8. X-ray photoelectron spectra of Au/TS-1 and TS-1 photocatalysts before and after the reaction. Au/TS-1: (a-1) Ti 2p and (a-2) Si 2p; TS-1: (b-1) Ti 2p and (b-2) Si 2p.

30.35 μmol.g^{-1}.h^{-1}, an improvement of 28% comparing with that of TS-1. However, in the case of Au/TiO_2 photocatalyst, most of C_3H_6 is still converted to CO_2 (75.1% selectivity). In this study, the percentage of C_3H_6 conversion is in the range of 0.02–0.03%.

Figure 10 shows the time-dependent behaviour of selectivity for the formation of various products over TS-1 and Au/TS-1 photocatalysts. At the initial stage of the reaction, very high acetaldehyde (AA) selectivity (70% and 55%) can be obtained. It then decreases and reaches steady state at 20% and 10% for TS-1 and Au/TS-1, respectively. The initial increase in AA selectivity is probably due to the presence of large amount of multi-coordinated Ti centres (Ti-O-Ti) in TS-1 support at the beginning. Stangland *et al.*[28] mentioned that when decrease in Ti-O-Ti entities occur, significant improvement in selectivity towards epoxide will result due to the reduced cracking of propylene to AA. This result further supports the enhanced reliability observed for the photocatalyst. In addition, only photocatalysts with TS-1 support can provide relatively good stability in the selective epoxidation for a period of over 12–15 h to give PO selectivity of 43.7% and 54.3% for TS-1 and Au/TS-1, respectively. Moreover, a very stable product distribution is achieved for both photocatalysts after 3 h of reaction.

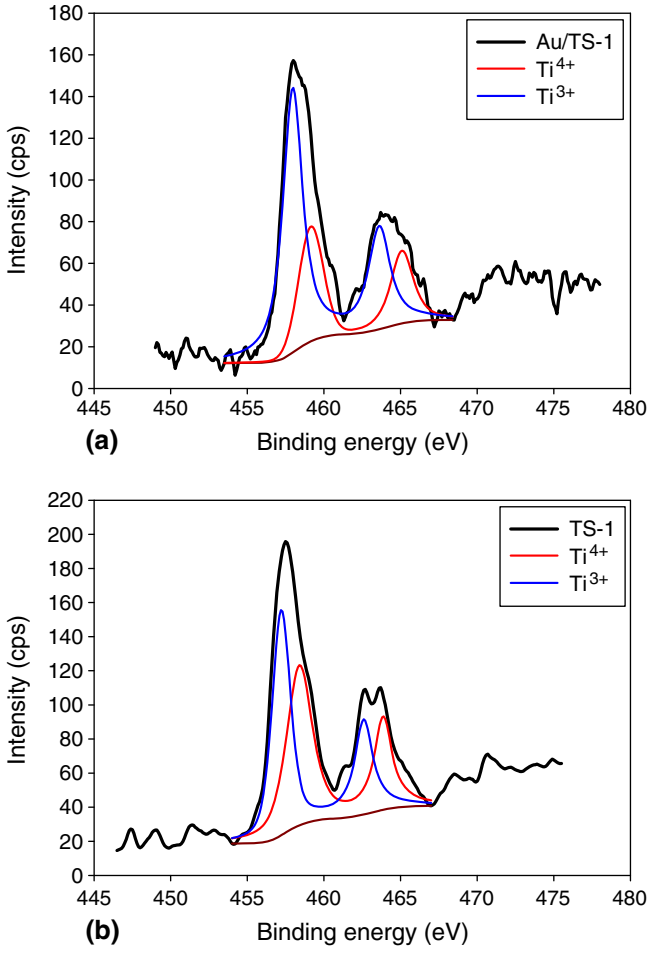

Figure 9. XPS spectra showing Ti 2p XPS peaks for (**a**) Au/TS-1 and (**b**) TS-1 photocatalysts. The spectra also show Ti^{3+} and Ti^{4+} peaks.

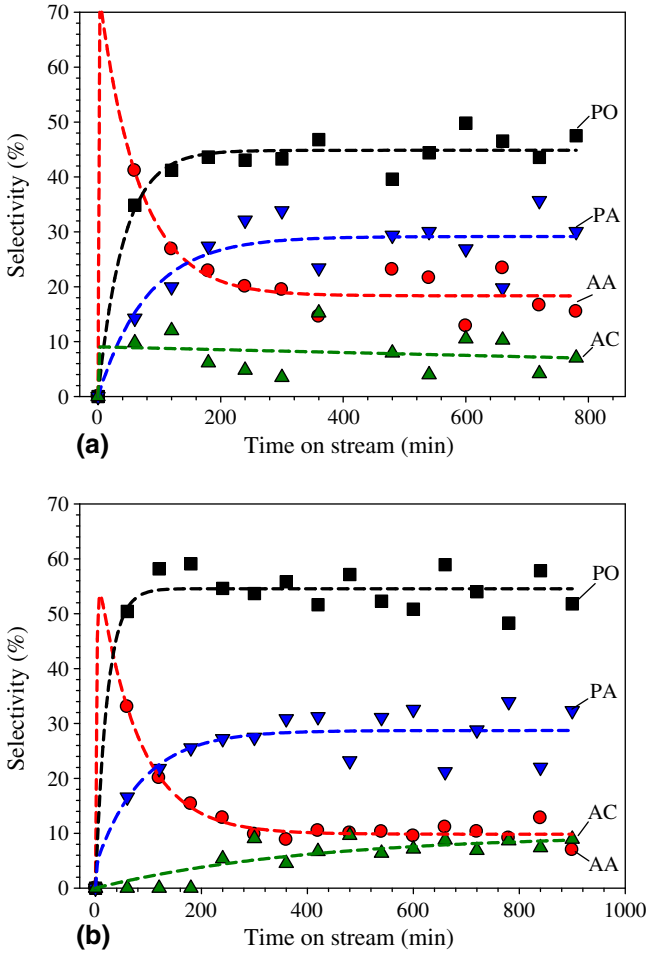

Figure 10. The time-dependent behaviour of selectivity for the formation of propylene oxide (PO), propionaldehyde (PA), acetaldehyde (AA) and acetone (AC) over (**a**) TS-1 and (**b**) Au/TS-1 photocatalysts at 323 K, 0.1 mW.cm–2.

It has been known that the major drawback of Au-loaded photocatalyst, which is effective in epoxidation, is its fast deactivation.[5] However, Au/TS-1 photocatalyst still shows good stability in propylene conversion rate (60 μmol.g^{-1}.h^{-1}) after 15 h of reaction as shown in figure 11, which is in agreement with the XPS results reported previously. We have mentioned that the Ti^{3+} sites in photocatalysts, which favour selective photo-epoxidation, are highly stable in air under irradiation and will not induce any activity degradation. As a result, good stability in C_3H_6 conversion can be achieved. This also implies that Au plays a crucial role in photo-epoxidation over the Au/TS-1 photocatalyst.

Recently, many studies have agreed that hydroperoxide intermediate species, which is responsible for selective epoxidation, are formed in the epoxidation of propylene using H_2–O_2 mixtures over Au-loaded photocatalysts.[3,5,13,16] The key factor determining the selective epoxidation reaction is the size of Au particles, i.e., very small Au particles (2–5 nm) are the most

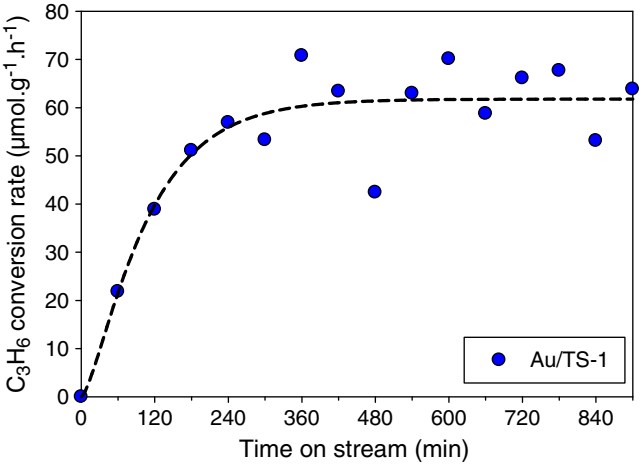

Figure 11. Time-dependent behaviour of C_3H_6 conversion rate over Au/TS-1 photocatalyst at 323 K, 0.1 mW.cm^{-2}.

active due to the high coverage of oxygen or oxygen-derived species, whereas large Au particles (> 5 nm) are less active and tend to cause complete combustion of C_3H_6 to CO_2.[5,29] In this study, we have shown that noble metal loaded photocatalysts can exhibit good selectivity towards epoxide formation in the presence of only molecular oxygen. However, contributions of Au in epoxidation without a sacrificial reductant such as H_2 are still a matter of debate.[30] Rojluechai *et al.*[31] suggested that oxygen species, which is responsible for selective epoxidation, are formed at the interface of Au particles and the supports.[31] In this case, larger the size of Au particles (≥ 2 nm), the more active sites the Au particles can provide to generate active oxygen species, which is in agreement with our results. For instance, photocatalyst with large Au particles (10–12 nm) can enhance selective epoxidation performance by providing more active sites for propylene epoxidation.

4. Conclusion

Au-loaded TiO_2 and TS-1 photocatalysts are successfully prepared and fully characterized. We found that the Au/TS-1 photocatalysts not only exhibit enhanced selectivity towards epoxide formation (54.3% selectivity), but also show improved stability in C_3H_6 conversion in which the products generated do not vary significantly with time. The enhancement in PO selectivity is due to the reduced cracking of propylene to AA, while the improvement in C_3H_6 conversion stability is due to the presence of highly stable Ti^{3+} sites, which will not induce any activity degradation. After 3 h of reaction, a very stable distribution of products can be achieved for both TS-1 and Au/TS-1 photocatalysts.

Acknowledgements

This research was financially supported by the National Science Council of Taiwan under contract number NSC 99-2923-E-002-002-MY2. The authors also thank Dr. Janusz Lasek from Institute for Chemical Processing of Coal, Poland for great help in designing the photo-reactor.

References

1. Nijhuis T A, Makkee M, Moulijn J A and Weckhuysen B M 2006 *Ind. Eng. Chem. Res.* **45** 3447
2. Trent D L 2000 In *Kirk–Othmer encyclopedia of chemical technology* (Hoboken, NJ: John Wiley & Sons, Inc)
3. Kahlich D, Wiechern U and Lindner J 2000 *Ullmann's encyclopedia of industrial chemistry* (Wiley-VCH Verlag GmbH & Co. KGaA)
4. *WP coverage of propylene oxide* 2011 World Petrochemicals
5. Joshi A M, Taylor B, Cumaranatunge L, Thomson K T and Delgass W N 2008 In *Mechanisms in homogeneous and heterogeneous epoxidation catalysis*, Oyama S T (ed) chapter 11 (Amsterdam: Elsevier) p 315
6. Hayashi T, Tanaka K and Haruta M 1998 *J. Catal.* **178** 566
7. Cumaranatunge L and Delgass W N 2005 *J. Catal.* **232** 38
8. Nijhuis T A, Huizinga B J, Makkee M and Moulijn J A 1999 *Ind. Eng. Chem. Res.* **38** 884
9. Taylor B, Lauterbach J and Delgass W N 2005 *Appl. Catal. A* **291** 188
10. Wang R, Guo X, Wang X, Hao J, Li G and Xiu J 2004 *Appl. Catal. A* **261** 7
11. Nguyen V-H, Chan H-Y, Wu J C S and Bai H 2012 *Chem. Eng. J.* **179** 285
12. Nguyen V-H, Wu J C S and Bai H 2013 *Catal. Commun.* **33** 57
13. Amano F, Tanaka T 2005 *Catal. Commun.* **6** 269
14. Amano F, Tanaka T 2006 *Chem. Lett.* **35** 468
15. Yoshida H, Murata C and Hattori T 2000 *J. Catal.* **194** 364
16. Khomane R B, Kulkarni B D, Paraskar A and Sainkar S R 2002 *Mater. Chem. Phys.* **76** 99
17. Yang Y-F, Sangeetha P and Chen Y-W 2009 *Int. J. Hydrogen Energy* **34** 8912
18. Ivanova S, Pitchon V, Petit C, Herschbach H, Dorsselaer A V and Leize E 2006 *Appl. Catal., A* **298** 203
19. Zhang W F, He Y L, Zhang M S, Yin Z and Chen Q 2000 *J. Phys. D: Appl. Phys.* **33** 912
20. Bordiga S, Damin A, Bonino F, Ricchiardi G, Zecchina A, Tagliapietra R and Lamberti C 2003 *Phys. Chem. Chem. Phys.* **5** 4390
21. Link S and El-Sayed M A 1999 *J. Phys. Chem. B* **103** 8410
22. Vayssilov G N 1999 *Cat. Rev.* **39** 209
23. Reddy M K, Manorama S V and Reddy A R 2003 *Mater. Chem. Phys.* **78** 239
24. Vetter S, Schulz-Ekloff G, Kulawik K and Jaeger N I 1994 *Chem. Eng. Technol.* **17** 348
25. Naik B, Parida K M and Gopinath C S 2010 *J. Phys. Chem. C* **114** 19473
26. Sinha A K, Seelan S, Tsubota S and Haruta M 2004 *Top. Catal.* **29** 95
27. Zuo F, Wang L, Wu T, Zhang Z, Borchardt D and Feng P 2010 *J. Am. Chem. Soc.* **132** 11856
28. Stangland E E, Taylor B, Andres R P and Delgass W N 2005 *J. Phys. Chem. B* **109** 2321
29. Lu J, Zhang X, Bravo-Suárez J J, Bando K K, Fujitani T and Oyama S T 2007 *J. Catal.* **250** 350
30. Suo Z, Jin M, Lu J, Wei Z and Li C 2008 *J. Nat. Gas Chem.* **17** 184
31. Rojluechai S, Chavadej S, Schwank J W and Meeyoo V 2007 *Catal. Commun.* **8** 57